Int. J. Electrochem. Sci., 7 **(2012)** 8128 - 8139

International Journal of
ELECTROCHEMICAL
SCIENCE
www.electrochemsci.org

A Study of Electrochemical Performance of $LiFePO_4$/C Composites Doped with Na and V

Ya-Wen Chen, Jenn-Shing Chen[*]

Department of Applied Chemistry, National University of Kaohsiung, Kaohsiung City, Taiwan 811, R.O.C.
[*]E-mail: jschen@nuk.edu.tw

Received: 13 July 2012 / *Accepted:* 8 August 2012 / *Published:* 1 September 2012

Metal-doping was applied to modify the electrochemical performance of olivine type $LiFePO_4$, for use as a cathode material. In this work, $LiFePO_4$/C, Na-doped $LiFePO_4$/C, V-doped $LiFePO_4$/C and Na,V-doped $LiFePO_4$/C composites were synthesized using the sol-gel method. All samples were characterized using inductively coupled plasma (ICP), X-ray diffraction (XRD), scanning electron microscopy (SEM), transmission electron microscopy (TEM), BET surface area, cyclic voltammetry (CV), electrochemical impedance spectroscopy (EIS) and charge-discharge tests. ICP and XRD analyses indicated that the sufficient doping of Na and V ions in $LiFePO_4$ was not to alter its crystal structure, but to slightly change the lattice parameters, which facilitates the diffusion of Li^+ ions and decreases the resistance to Li ions and electron transfer on the electrode. The doped samples exhibit better high-rate and cycle performances than the un-doped $LiFePO_4$/C. The electrochemical performance depends on the different ionic dopants used to prepare the electrode. The V-doped sample outperformed all other samples, because doping with a V cation, which has a greater intrinsic conductivity, confers the sample with smaller charge-transfer resistance and better kinetic behavior.

Keywords: $LiFePO_4$, Lithium-ion batteries, Cathode material, Na-Doping, V-Doping

1. INTRODUCTION

Olivine $LiFePO_4$ has been widely studied and is a good candidate for a cathode material for Li-ion batteries, because of its high theoretical capacity (170 mAh/g), cycling stability, low cost and environmental friendliness. These attractive characteristics make olivine $LiFePO_4$ highly suitable for use in large-scale Li-ion batteries for electric vehicles (EV) and hybrid electric vehicles (HEV). However, its poor performance has limited its applications. The major reason for its poor performance is its low electronic conductivity and the sluggish Li^+ diffusion that occurs across the $LiFePO_4$/$FePO_4$

interface [1-3]. In order to overcome these problems, several strategies have been used over the years, from optimized synthesis procedures [4,5], carbon nanocoating [6,7], particle-size minimization [8] and metal powder addition [9,10], to doping with alien cations [11] or the carbothermal formation of the surface conducting phase [11-14]. Of these methods, doping alien cations is considered the most effective in improving the electronic conductivity and Li-ion diffusion rate [15-25]. Recently, many elements have been used to dope $LiFePO_4$ at the Li-site in $Li_{1-x}M_xFePO_4$ (M = Zr, Nb, Cr, Cu, Ti, Mo, Mg, Na etc.) [15-18]. However, the performance of the material doped with a high valence metal ion did not meet expectations [15-25]. $LiFePO_4$ has a one-dimensional lithium ion diffusion pathway, during the charge-discharge process, and doping with high valence transition metal ions at the Li site in the $LiFePO_4$ blocks the one-dimensional diffusion pathway, which results in lower ionic conductivity. Some experimental and theoretical results show that the electronic conductivity is enhanced and that the improved ionic transport allows better performance for a Na-doped (Li site) $LiFePO_4$ [15-17]. Similarly, many studies have shown that Fe^{2+} doping with "supervalent" metal ions, namely $LiFe_{1-x}M_xPO_4$ (Ni, Co, Al, V, etc.), can effectively stabilize the crystal structure and cause a slight increase in the intrinsic electronic conductivity [18-25]. Recently, several studies have suggested that $LiFe_{1-x}V_xPO_4$, in which the Fe-site is occupied by vanadium, improves the performance of $LiFePO_4$, especially on the aspect of a stable cycle-life at a high C rate [23]. Although many doping alien cations have been used effectively to improve the electronic conductivity, the effects of doping both the Li and Fe sites with two alien cations requires further study, as few reports are presented in literatures. Therefore, with due respect to the available literature on studies concerning doping with various metal ions, this work uses Na and V metals as alien cations for the preparation of Na-doped $LiFePO_4$/C, V-doped $LiFePO_4$/C and Na,V-doped $LiFePO_4$/C composites.

In order to clarify the effect of doping with alien cations on $LiFePO_4$ composites, the sol-gel method was used to prepare $LiFePO_4$ and its carbon composites, because of its simplicity and low cost. Moreover, it is simple to control the amount and characteristics of the residual carbon on the surface of the $LiFePO_4$ particles. The physicochemical properties and electrochemical behavior of the samples were characterized.

2. EXPERIMENTAL PART

2.1 Material preparation

$LiFePO_4$/C and Na,V-doped $LiFePO_4$/C composites were synthesized via a sol-gel preparation route. Accordingly, $LiOH•H_2O$ (TEDIA), $Fe(NO_3)_3•9H_2O$ (Riedel-deHaen), H_3PO_4 (J.T. Baker), and Citric Acid (TEDIA) and Na_2CO_3 (J.T. Baker) or NH_4VO_3 (Sigma-Aldrich) were used as reactants. The stoichiometric amounts of reactants were dissolved in deionized water. The mixed solution was heated and maintained at 75℃ in a thermostatic bath under uniform stirring until a viscous gel was formed. The gel was dried in an oven at 100℃ for 12 h and then was calcined in a tubular furnace at 700℃ for 8 h under reducing atmosphere (Ar/H_2 = 95/5) to yield $LiFePO_4$/C, Na-doped $LiFePO_4$/C, V-doped $LiFePO_4$/C, and Na,V-doped $LiFePO_4$/C composite materials.

2.2 Analytical characterization

A Rigaku-D/MaX-2550 diffractometer, with Cu K_α radiation (λ=1.54 Å), was used to obtain X-ray diffraction (XRD) patterns for the samples. The morphology of the sample was observed using a scanning electron microscopy (SEM, Hitachi S-4300) and a transmission electron microscopy (TEM, JEOL JEM-2010). The V or Na ion content was determined using inductively coupled plasma (ICP, Optima 2100DV). The Brunauer-Emmett-Teller (BET) method was used to measure the specific surface area of powders (ASAP2020). The residual carbon content of the powders was determined by means of an automatic elemental analyzer (Elementar vario, EL III).

2.3 Electrochemical characterization

For electrochemical evaluation, the composite electrodes were prepared by wet coating, and were fabricated using as-prepared $LiFePO_4$/C with acetylene black, SFG-6 synthetic flake graphite (Timcal Ltd.) and poly(vinylidene difluoride) (PVdF) binder (MKB-212C, Elf Atochem), in a weight ratio of 80:5:5:10. The $LiFePO_4$/C active materials, acetylene black and SFG-6 were first added to a solution of PVdF in N-methyl-2-pyrrolidone (NMP, Riedel-deHaen). The mixture was stirred for 20 min at room temperature with a magnetic bar, and then with a turbine for 5 min at 2000 rpm to make a slurry with an appropriate viscosity. The resulting slurry was coated onto a piece of aluminum foil and dried at 120^{o}C for 40 min. The coating had a thickness of ~100 μm, with an active material mass loading of 8 ± 1 mg cm^{-2}. The quantity of active materials on the electrodes was maintained at a constant level. The electrodes were dried overnight at 100^{o}C under vacuum before being transferred to an argon-filled glove box for cell assembly. The electrodes were placed in an open glass bottle cell with a 1 cm^2 square $LiFePO_4$/C cathode and lithium foil as the counter and reference electrodes for the CV experiment. Coin cells of size 2032 were assembled using lithium metal as a counter electrode. A solution of 1 M $LiPF_6$ in a mixed solvent of ethylene carbonate/dimethyl carbonate (EC/DMC) with a 1:1 volume ratio was used as the electrolyte in all cells. The CV experiment was carried out with a CHI 704A potentiostat at a scan rate of 0.1 mV s^{-1}. During EIS measurement, the excitation voltage applied to the cells was 5 mV and the frequency range was between 100 kHz and 10 mHz. The coin cells were cycled galvanoststically with a BAT-750B (Acu Tech System), using a constant current of 0.5C and a voltage of 2.5–4.2 V vs. Li/Li^+ at room temperature; here, 1C equals 170 mA g^{-1}. The current density was calculated based on the mass of active material in the electrode.

3. RESULTS AND DISCUSSION

The target molar ratio of Li:Na:Fe:V:P in the sample was 0.97:0.03:0.97:0.03:1.00. The ICP results for the undoped and doped compounds are shown in Table 1. It is clear that both the Na and V content of the doped compounds are close to the target values, which shows that this method can accurately maintain a given content for the dopant. All of the prepared undoped and doped $LiFePO_4$/C

powders were deep black in color, in contrast to the gray color of pure $LiFePO_4$ powder. Fig. 1 shows the XRD patterns of the prepared samples.

Table 1. Elemental content of the prepared samples, as determined using ICP*.

Sample	Li	Na	Fe	V	P
$LiFePO_4$/C	1.03(4)	-	1.00(1)	-	1
Na-doped $LiFePO_4$/C	0.97(7)	0.01(9)	1.02(3)	-	1
V-doped $LiFePO_4$/C	1.01(5)	-	0.97(1)	0.02(4)	1
Na, V-doped $LiFePO_4$/C	0.99(0)	0.02(1)	0.98(1)	0.02(5)	1

* molar ratio and based on element P as 1.

Table 2. Lattice parameters of the prepared samples.

Sample	*a* (Å)	*b* (Å)	*c* (Å)	*V* (Å^3)
$LiFePO_4$/C	10.2792	5.9939	4.6743	287.9952
Na-doped $LiFePO_4$/C	10.3020	5.9905	4.6858	289.1801
V-doped $LiFePO_4$/C	10.2697	5.9736	4.6870	287.5338
Na, V-doped $LiFePO_4$/C	10.3233	5.9759	4.6881	289.2136

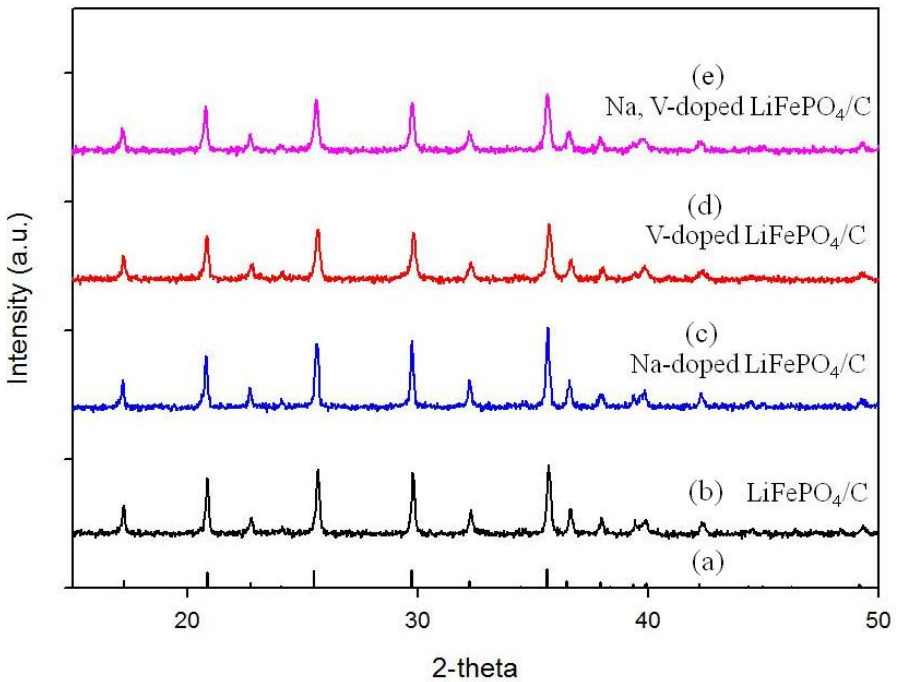

Figure 1. XRD patterns of (a) theoretical pattern, (b)$LiFePO_4$/C, (c)Na-doped $LiFePO_4$/C, (d)V-doped $LiFePO_4$/C and (e)Na, V-doped $LiFePO_4$/C.

All of the peaks can be attributed to a pure and well-crystallized $LiFePO_4$ phase, with an ordered olivine structure, indexed to the orthorhombic *Pnmb* space group. There are no peaks, but reflections were found in the diffractograms of carbon in the final product, which indicates that the carbon generated by the pyrolysis of citric acid is amorphous in the final product. This is reasonable, because the content of the residual carbon for all prepared samples was approximately 2 - 3wt.%, as determined by elemental analyzer (EA). Moreover, doping with Na and V does not destroy the lattice structure of $LiFePO_4$ because of the low doping concentration. Table 2 shows the cell parameters for the samples, as calculated using XRD analysis. As can be seen, the Na and V dopants have been successfully doped into the Li and Fe sites, without destroying the lattice structure, but there is a slight change in the lattice parameters. The cell parameters for the undoped $LiFePO_4$/C sample are a=10.2792Å, b=5.9939Å, c=4.6743Å and the unit cell volume = 287.9952Å^3. It is found that Na-doped $LiFePO_4$/C elongates the a and c axes and shrinks the b axis, but enlarges the lattice volume. The doped Na is inclined to occupy Li sites, because the $NaFePO_4$ has a similar structure to $LiFePO_4$ and the Na ion (r=0.97Å) has larger radius than that of the Li ion (r=0.68Å) in the octahedral, which causes a change in the lattice parameters. A smaller b value shortens the diffusion distance for the Li ion and causes an increase in the rate of Li^+ diffusion [15]. V doping decreases the values of a and b, but increases the value of c and the lattice volume. Except for the benefit of smaller b value, the substitution of Fe by V results in an increase in the Li-O bond length, due to a smaller bond energy, which improves the Li^+ intercalation/de-intercalation [25]. The change in lattice parameters for the Na,V-doped $LiFePO_4$/C is similar to that for Na-doped $LiFePO_4$/C. Doping with Na causes a greater change in the lattice parameters for Na,V-doped $LiFePO_4$/C than doping with V . In addition, the total unit cell volume for Na-doped $LiFePO_4$/C and Na,V-doped $LiFePO_4$/C are enlarged. The expansion in the crystal lattice allows more space for the insertion and removal of Li^+. The greater change in the lattice parameters and more increase in cell volume associated with the Na dopant is probably attributable to the larger radius of the Na ion, compared to those of the Li, Fe and V ions.

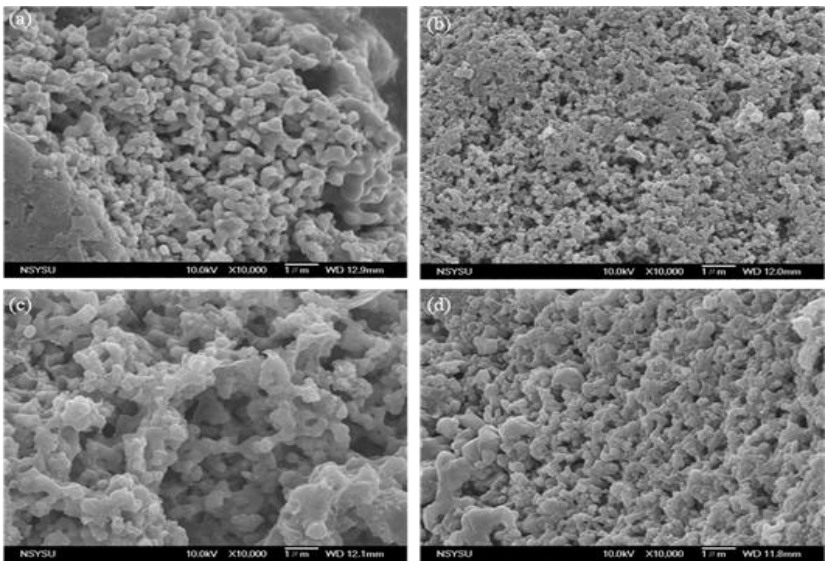

Figure 2. SEM images of (a) $LiFePO_4$/C, (b)Na-doped $LiFePO_4$/C, (c)V-doped $LiFePO_4$/C and (d)Na, V-doped $LiFePO_4$/C.

The morphology of $LiFePO_4$/C and $LiFePO_4$/C doped with ion powders was observed using SEM, as shown in Fig. 2. The general appearance of the grains in all samples is well proportioned and the size is narrowly distributed around 0.1-0.3μm, although a few agglomerates exist. The composites appear to be framed by an amorphous carbon matrix, which contains the $LiFePO_4$ particles.

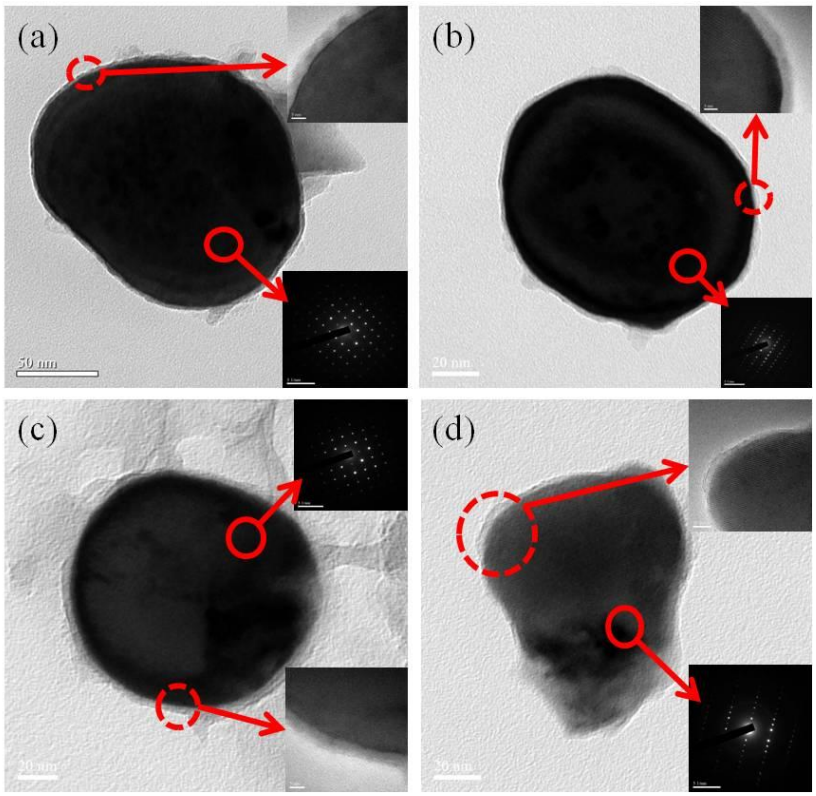

Figure 3. TEM images of (a) $LiFePO_4$/C, (b)Na-doped $LiFePO_4$/C, (c)V-doped $LiFePO_4$/C and (d)Na, V-doped $LiFePO_4$/C. The inserts are SAED patterns and high-resolution TEM images of the circled regions, respectively.

Fig. 3 shows the TEM images of $LiFePO_4$/C and $LiFePO_4$/C composites doped with ions. The inserts in Fig.3 show diffraction patterns for the particles and web in selected areas, in which the crystal of $LiFePO_4$ appears dark and the carbon coating appears gray (marked with a dashed circle). Obviously, the entire carbon distribution surrounds the fine $LiFePO_4$ crystal grains like a web made of carbon. This "carbon web" results in electronic inter-grain connection, but does not block the direct contact between the active particles and the encapsulated electrolyte. As shown in Fig.3, the particle size of the $LiFePO_4$ is between 100-200 nm and the thickness of the carbon coating is approximately 5 nm. Table 3 presents the residual carbon content, particle size and BET surface area for all of the samples prepared from $LiFePO_4$/C and $LiFePO_4$/C composites doped with ions. In order to ensure that there were equal amounts of residual carbon in the composites, the final content of the residual carbon of all of the samples was maintained at approximately 2 – 3wt.%. Taken together, the data in table 3 verifies that the composites doped with ions have smaller particle size, which results in a larger surface area. The particle size decreases, which is consistent with the increase in the specific surface

area, from 14.89, 17.54, 22.29 and 25.40 $m^2 g^{-1}$, for the $LiFePO_4$/C, Na-doped $LiFePO_4$/C, V-doped $LiFePO_4$/C and Na,V-doped $LiFePO_4$/C, respectively.

Table 3. Comparison of the residual carbon content, particle size and surface area, for all of the prepared samples.

Samples	Residual carbon content (wt%)	Particle sizes* (nm)	BET surface area (m^2g^{-1})
$LiFePO_4$/C	2.49	175	14.89
Na-doped $LiFePO_4$/C	2.06	117	17.54
V-doped $LiFePO_4$/C	2.97	117	22.29
Na,V-doped $LiFePO_4$/C	2.91	109	25.40

* From TEM images

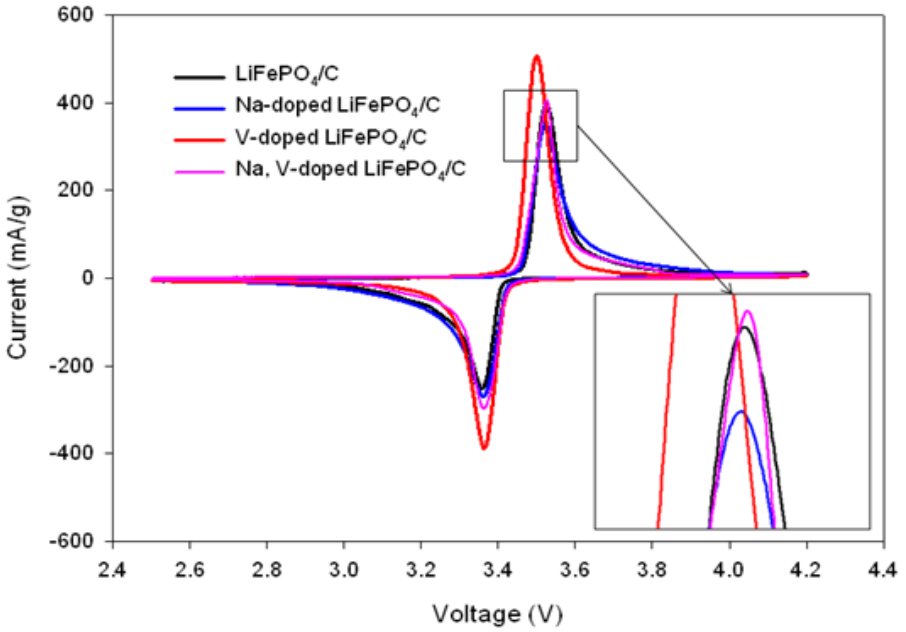

Figure 4. CV profile of the prepared samples, using a scan rate of 0.1 mV/s, from 2.5 V to 4.2 V.

The CV plots for different $LiFePO_4$/C electrodes in a beaker cell, cycled between 3.0 and 4.0 V at 0.1mV s^{-1} and using 1M $LiPF_6$ + EC/DMC (1:1) electrolyte, are shown in Fig. 4. The CV curves of all samples exhibit two peaks, which are located at 3.5 V in the anodic sweep and 3.3 V in the cathodic sweep; these are consistent with a two-phase redox reaction at about 3.5 V vs. Li/Li^+. No other peaks are present, which indicates an absence of electroactive iron impurities. In addition, the peak potential separations are 0.167, 0.162, 0.138 and 0.163 V for the $LiFePO_4$/C, Na-doped $LiFePO_4$/C, V-doped $LiFePO_4$/C and Na,V-doped $LiFePO_4$/C, respectively. The V-doped $LiFePO_4$/C has a narrower peak potential separation and a larger current peak (Insert in Fig.4), which indicates the best reversibility of the electrode reaction and the best kinetic behavior.

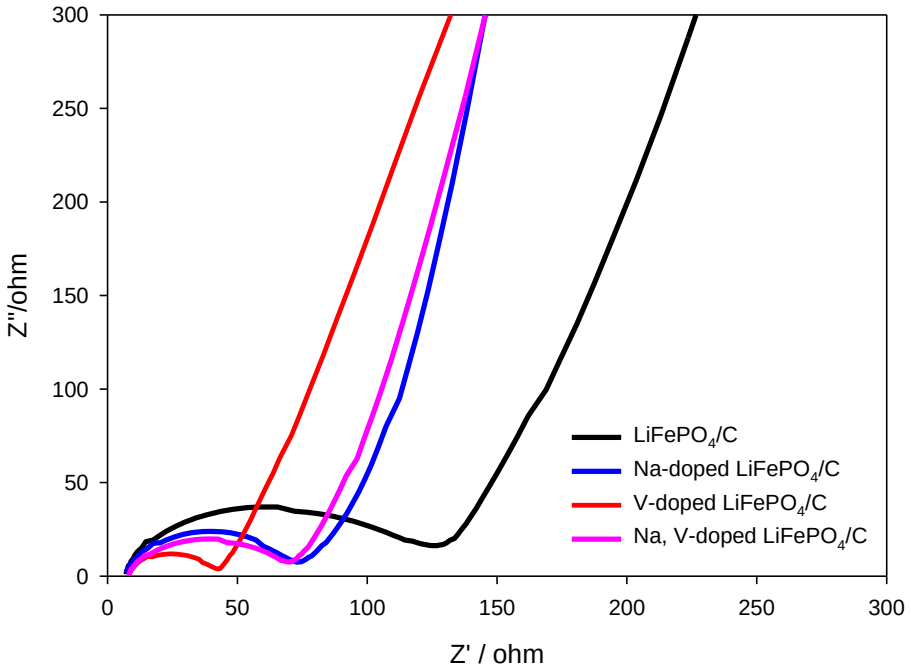

Figure 5. A.C. impedance spectra of the prepared samples.

Electrochemical impedance spectroscopy was measured on the coin cells in the fully charge state. Fig.5 shows the typical Nyquist plots for the spectra of all of the prepared samples. All of the spectra have an intercept at high frequency, followed by a semicircular plot in the medium-to-high frequency region and a sloping line in the low frequency region. The intercept at the Z' axis in the high frequency region corresponds to the ohmic resistance (R_e) of the electrolyte and the electrical contact. The semicircular plot in the medium frequency range is attributable to the charge transfer resistance (R_{ct}) of the electrochemical reaction and the sloping line in the low frequency region represents the diffusion of lithium ions into the bulk of the cathode material, namely the Warburg impedance [26,27]. As indicated in Fig.5, the R_{ct} values for $LiFePO_4$/C, Na-doped $LiFePO_4$/C, V-doped $LiFePO_4$/C and Na,V-doped $LiFePO_4$/C, are 119, 65, 34 and 61 Ω, respectively. It is seen that the Na and V dopants in the $LiFePO_4$/C composites cause a decrease in the resistance to charge-transfer and an increase in the Li ion diffusion coefficient. Generally, the decrease in the resistance to charge-transfer indicates that Li ion and electron transfer are more feasible at the electrode, which is beneficial to the kinetic behavior during charge-discharge process, thereby producing an improvement in electrochemical performance. Furthermore, the V-doped $LiFePO_4$/C composite exhibits the smallest charge-transfer resistance of the four samples. Therefore, it is expected that the V-doped $LiFePO_4$/C should have excellent kinetic behavior, which is consistent with the CV measurement shown in Fig.4. Also, as shown in Fig.5, the slope of the line in the low frequency region increases as the Na and V dopants in the $LiFePO_4$/C composites and the effect is greater for doping with Na. As seen in the results of XRD analysis, in Table 2, Na doping results in a smaller *b* value, which abbreviates the diffusion distance for the Li ion and causes an increase in the rate for the diffusion of the Li^+ ion.

Therefore, the Na-doped $LiFePO_4/C$ exhibits the greatest rate of lithium ion diffusion into the $LiFePO_4$ particles.

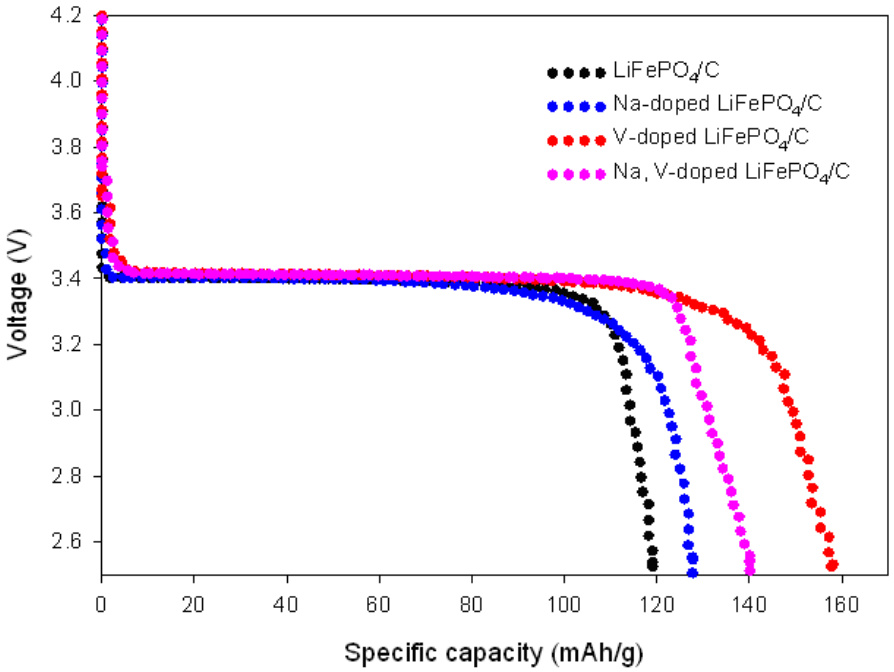

Figure 6. The 15th discharge curves of the cells for all samples at 0.1C rate.

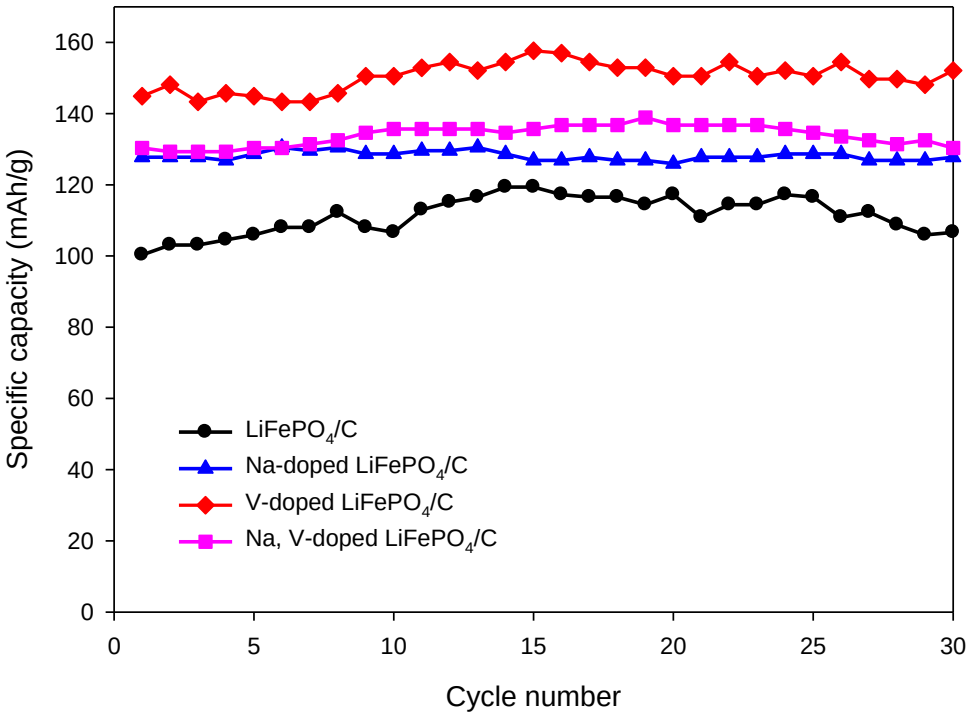

Figure 7. The capacity retention of the LiFePO4/C samples cycled at 0.1C rate between 2.5 and 4.2 V.

Fig. 6 shows the discharge voltage profiles of the Li/$LiFePO_4$ cells for all samples at a 0.1 C rate during the 15th cycle. It can be seen that all of the samples display similar discharge curves with a potential plateau over a wide voltage range at approximately 3.4 V (vs. Li/Li^+). This implies that a two-phase Fe^{3+}/Fe^{2+} redox reaction proceeds via a first-order transition between $FePO_4$ and $LiFePO_4$. The specific discharge capacity of $LiFePO_4$/C, Na-doped $LiFePO_4$/C, V-doped $LiFePO_4$/C and Na,V-doped $LiFePO_4$/C is 119, 130, 158, and 139 mAh g^{-1}, respectively. Obviously, the doped $LiFePO_4$/C exhibits better electrochemical performance. This is completely consistent with the results from CV and EIS. The V-doped $LiFePO_4$/C delivers the highest discharge capacity of 158 mAh g^{-1}, which is approximately 93% of the theoretical capacity (170 mAh g^{-1}). The V-doped sample, with lesser resistance to charge-transfer and better kinetic behavior, has a higher capacity than the Na-doped sample. Therefore, the effect of resistance to charge-transfer or electric conductivity on the discharge capacity at a lower rate of discharge is more important than that of the lithium ion diffusion in $LiFePO_4$. Fig. 7 shows a plot of discharge capacity versus cycle number for Li/$LiFePO_4$ cells from different samples. All of the cells display stable cycle performance over 30 consecutive cycles. The cell discharge capacity has a strong relationship with the alien cations. The V-doped sample outperforms all of the other samples, because doping with a V cation, which has a larger intrinsic conductivity, confers the sample with lesser resistance to charge-transfer and better kinetic behavior. The cycle stability of all samples at various rates of discharge current is presented in Fig. 8.

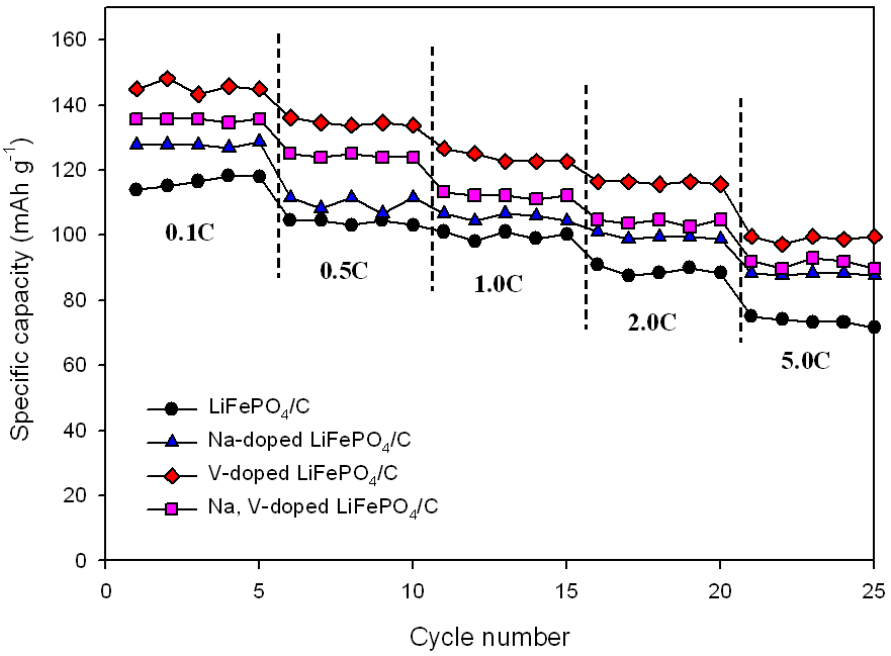

Figure 8. The cycle performance for the half-cell for all samples, measured at different rates of discharge.

All of the samples show good capacity for reversal of the cycle with little diminution of capacity at each current density. However, discharge capacity decreases as the discharge rate is

increased, which indicates that rate limitations remain. At a rate of 5C, a reversible discharge capacity of approximately 63%, 69%, 68% and 67% of the initial capacity is achieved at a 0.1C rate, for $LiFePO_4$/C, Na-doped $LiFePO_4$/C, V-doped $LiFePO_4$/C and Na,V-doped $LiFePO_4$/C, respectively. The rate of this decrease is less for the Na-doped $LiFePO_4$/C than for the other samples, which is attributable to the decrease in lithium ion diffusion in $LiFePO_4$ particles. Therefore, because of this increase in the intrinsic conductivity and the increase in the rate of diffusion of the Li^+ ion, the Na or V doped $LiFePO_4$/C ($Li_{1-x}Na_xFePO_4$/C, $LiFe_{1-y}V_yPO_4$ and $Li_{1-x}Na_xFe_{1-y}V_yPO_4$/C) composites exhibit better electrochemical performance than undoped $LiFePO_4$/C composite.

4. CONCLUSIONS

Well crystallized powders of $LiFePO_4$/C, doped with V and Na cations, were prepared using the sol-gel method and investigated using ICP, XRD, SEM, TEM, EA, BET, CV, EIS and charge-discharge tests. These show that a low amount of Na and V cations doped into the Li and Fe sites does not destroy the lattice structure, but slightly changes the lattice parameters, which facilitates the diffusion of the Li^+ ion and decreases the resistance of the Li ion and electron transfer on the electrode.

It is clear that the doped samples exhibit a higher discharge capacity. The cell discharge capacity and rate capacity depends on the type of ion used to dope the electrode. CV and EIS examination confirmed these results. Obviously, the Na or V doped $LiFePO_4$/C ($Li_{1-x}Na_xFePO_4$/C, $LiFe_{1-y}V_yPO_4$ and $Li_{1-x}Na_xFe_{1-y}V_yPO_4$/C) composites exhibit better electrochemical performance than the undoped $LiFePO_4$/C composite and this is attributable to a greater electronic conductivity and larger coefficient for the diffusion of the Li^+ ion.

ACKNOWLEDGMENTS
This authors thank the National Science Council of Taiwan for the financial support in this work under contract no. NSC 100-2113-M-390-003-.

References

1. A.K. Padhi, K.S. Nanjundaswamy, J.B. Goodenough, *J. Electrochem. Soc*. 144 (1997) 1188.
2. S.Y. Chung, J.T. Bloking, Y.M. Chiang, *Nat. Mater.* 2 (2002) 123.
3. K. Striebel, J. Shim, V. Srinivasan, J. Newman, *J. Electrochem. Soc.* 152 (2005) A664.
4. G. Arnold, J. Garche, R. Hemmer, S. Strobele, C. Vogler, M. Wohlfahrt-Mehrens, *J. Power Sources* 247 (2003) 119.
5. H. Huang, S.C. Yin, L.F. Nazar, *Electrochem. Solid State Lett*. 4 (2001) A170.
6. Z. Chen, J.R. Dahn, *J. Electrochem. Soc*. 149 (2002) A1184.
7. A. Yamada, S.C. Chung, K. Hinokuma, *J. Electrochem. Soc*. 148 (2001) A224.
8. F. Croce, A.D. Epifanio, J. Hassoum, A. Deptula, T. Olczac, B. Scrosati, *Electrochem. Solid-Sate Lett.* 5 (2002) 47.
9. K.S. Park, J.T. Son, H.T. Chung, S.J. Kim, C.H. Lee, K.T. Kang, H.G. Kim, *Solid State Commun*. 129 (2004) 31.

10. S.Y. Chung, J.T. Bloking, Y.M. Chiang, *Nat. Mater.* 2 (2002) 123.
11. P.S. Herie, B. Ellis, N. Coombs, L.F. Nazar, *Nat. Mater*. 3 (2004) 147.
12. M. Doeff, Y. Hu, F. McLarnon, R. Kostecki, *Electrochem. Solid State Lett*. 6 (2003) A207.
13. J.H. Lin, J.S. Chen, *Electrochim. Acta* 62 (2002) 461.
14. H.C. Wong, J.R. Carey, J.S. Chen, *Int. J. Electrochem. Sci*. 5 (2010) 968.
15. X. Yin, K. Huang, S. Liu, H. Wang, *J. Power Sources* 195 (2010) 4308.
16. M. Park, X. Zhang, M. Chung, G.B. Less, A.M. Sastry, *J. Power Sources* 195 (2010) 7904.
17. C.Y. Ouyang, S.Q. Shi, Z.X. Wang, H. Li, X.J. Huang, L.Q. Chen, *J. Phys. Condens. Matter*. 16 (2004) 2265.
18. J.B. Goodenough, Y. Kim, *Chem. Mater*. 22 (2010) 587.
19. B.L. Ellis, K.T. Lee, L.F. Nazar, *Chem. Mater*. 22 (2010) 691.
20. H. Liu, C. Li, Q. Cao, Y.P. Wu, R.J. Holze, *Solid State Electrochem*. 12 (2008) 1017.
21. C.S. Sun, Z. Zhou, Z.G. Xu, D.G. Wang, J.P. Wei, X.K. Bian, J. Yan, *J. Power Sources* 193 (2009) 841.
22. M.R. Yang, W.H. Re J. Electrochem. Soc. 155 (2008) A729.
23. D. Zhang, P. Zhang, J. Yi, Q. Yuan, J. Jiang, Q. Xu, Z. Luo, X. Ren, *J. Alloys Compd*. 509 (2011) 1206.
24. N. Hua, C. Wang, X. Kang, T. Wumair, Y. Han, *J. Alloys Compd*. 503 (2010) 204.
25. J. Ma, B. Li, H. Du, C. Xu, F. Kang, *J. Electrochem. Soc*. 158 (2011) A26.
26. H. Liu, Q. Cao, L.J. Fu, C. Li, Y.P. H.Q. Wu, H.Q. *Electrochem. Commun*. 8 (2006) 1553.
27. J. Molenda, W. Ojczyk, J. Marzec, *J. Power Sources* 174 (2007) 689.